

FULL TITLE
*ASP Conference Series, Vol. **VOLUME**, **YEAR OF PUBLICATION***
 NAMES OF EDITORS

Feeding the AGN with backflows

V. Antonuccio-Delogu^{1,2,3}, J. Silk²

¹*INAF - Osservatorio Astrofisico di Catania, Via S. Sofia 78, I-95123 Catania, ITALY*

²*Astrophysics, Department of Physics, University of Oxford, OX3 RH1 Oxford, UK*

³*Scuola Superiore di Catania, Via San Nullo, 5/i, I-95123 Catania, Italy*

Abstract. We study the internal circulation within the cocoon carved out by a relativistic jet emanating from an AGN, first developing model and then validating it using a series of numerical simulations. We notice that a significant increase of *circulation* in this flow arises because gradients in the density and entropy develop near the hot spot, as a consequence of Crocco's vorticity theorem. We find simple solutions for the streamlines, and we use them to predict the mass inflow rates towards the central regions. The 2D simulations we perform span a rather wide range of mechanical jet's input power and Black Hole masses, and we show that the predicted nuclear mass inflows are in good agreement with the theoretical model.

We thus suggest that these backflows could (at least partially) feed the AGN, and provide a self-regulatory mechanism of AGN activity, that is not directly controlled by, but possibly controls, the star formation rate within the central circumnuclear disk.

1. Introduction

The presence of compact objects (hereafter *Black Holes*, BHs) in the central dense regions of galaxies is often related to the AGN phenomenon. Moreover, since the original theoretical suggestion by Silk & Rees (1998), significant observational evidence has been accumulated concerning the impact of nuclear activity on the global stellar evolution within the host galaxy (see e.g. Schawinski et al. 2006; Yi et al. 2007; Kaviraj et al. 2007, 2008, for some recent work). In addition to its effect on *global* star formation, the presence of an AGN seems also to be connected with *circumnuclear starbursts* on small (from -parsec to kilo-parsec) scales (Storchi-Bergmann et al. 2001; González Delgado & Cid Fernandes 2005; Sarzi et al. 2007; Davies et al. 2007). However, despite all this observational evidence, the connection between AGN activity, negative/positive feedback on star formation, and local starbursts is not well understood.

If the main physical agent for this connection is the interaction between the jet and the host galaxy's interstellar medium (hereafter ISM), then it is important to model the physical consequences of the propagation of AGN relativistic jets into the ISM, and the mechanism which feeds the parsec-scale accretion

disc around the central BHs. Recent simulations (Sutherland & Bicknell 2007; Antonuccio-Delogu & Silk 2008) have begun to self-consistently model the feedback of a relativistic jet on its host galaxy, and the global consequences for e.g. blue-to-red cloud migration and downsizing (Tortora et al. 2009). Here we will focus our attention on the *large scale structure of the flow* within the cocoon, and on its consequences for the accretion onto the central BH.

2. Formation of the backflow

We distinguish 3 different sections in the circulation (see Fig. 1): propagation near the jet, then from the hotspot along the inner part of the bow shock, and along the meridional plane.

2.1. Model

Falle (1991) and Kaiser & Alexander (1997) have shown that a *recollimation shock* (hereafter RS) forms at some distance along the path of the jet. The post-shocked gas then accumulates into a region confined between the RS and the outer surface of the bow shock (see Figure 1), with a density $n_{hs} \approx 7n_j$, as appropriate to shocked, hot (relativistic) gas. We generically call this region the *hot spot* (HS).

Most of the cocoon is occupied by very low density, high temperature gas,

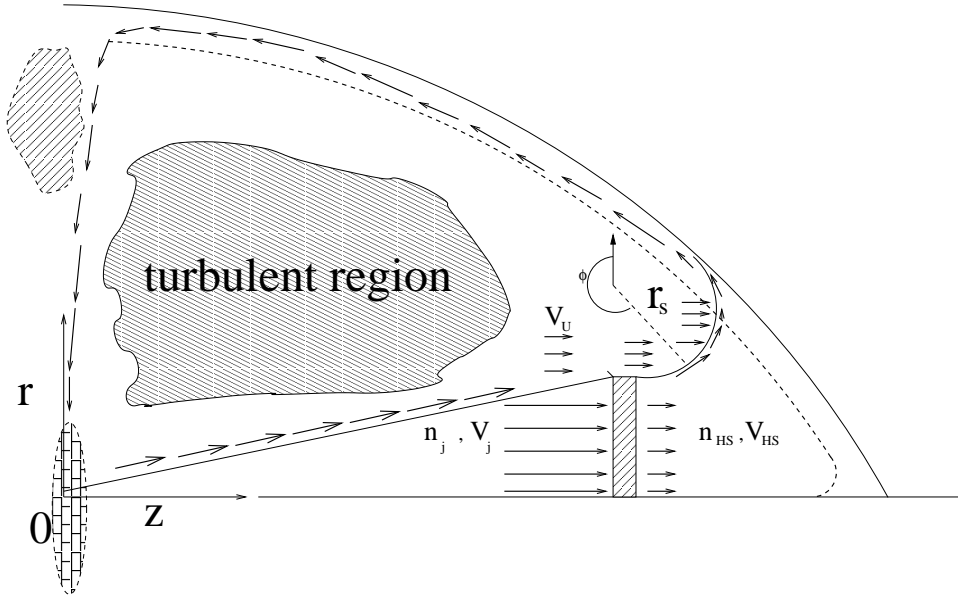


Figure 1. Schematic model of the origin of circulation near the hot spot and in the equatorial plane of the cocoon. We assume that the *hotspot* (HS) is bounded by a lateral spherical section having curvature radius r_s .

which keeps the jet pressure confined and collimated, even in the absence of magnetic fields. In this region the gas is in a turbulent state, with very little or no systematic motions. This region however does not extend directly down to

the boundary of the jet: the initial shear of the latter induces parallel motions of the gas near and outside the jet axis. This gas eventually reaches the HS, post-shocked region, where the density is significantly higher than in the cocoon. Obviously, the shocked gas within the hot spot has a higher entropy than that in the cocoon. Under these conditions, *Crocco's theorem* states that a circulation arises within a compressible fluid, even if in laminar motion (see Cap 2001, for a more recent discussion). In planar geometry the only component of the circulation is normal to the flow plane, and its magnitude is given by:

$$\omega v = T \frac{ds}{dn} - \frac{dh_0}{dn} \quad (1)$$

where: n is the normal to the direction perpendicular to the streamline, $\omega \equiv |\omega|$ is the modulus of the circulation, and s and $h_0 = h + v^2/2$ are the specific entropy and stagnation enthalpy, respectively.

2.2. Flow near the Hot Spot

We will approximate the recollimation shock surface before the hotspot as planar, thus the entropy is constant across the streamline, and the flow will not gain any circulation. However, the gas flowing *near and outside* the jet, will also eventually reach the HS: the boundary layer separating this region from the turbulent region will be a curved surface, joining the recollimation shock to the bow shock (see Fig. 1). We then assume that this off-axis flow motion is predominantly directed along the z - direction, thus: $\mathbf{v} \equiv v_{u|z} \hat{\mathbf{z}}$. Hereafter, subscripts u and d will denote quantities computed in the upstream and downstream regions, respectively, where by the latter we mean the HS, as shown in Figure 1. In order to compute ω_{hs} , the circulation in the hot spot, we will make use of the expression for the circulation near a curved shock, derived by Shapiro (1958, eq. 8):

$$\omega_{hs} = \frac{2v_{z|u}}{r_s(\gamma+1)} \frac{(M_n^2 - 1) |\cos \phi|}{M_n^2 [2 + (\gamma - 1) M_n^2]} \quad (2)$$

where: $M_n = (v_z/c_s) \cos \theta$ is the Mach number in the upstream flow region. As we show in Antonuccio-Delogu and Silk (2009, submitted) one can obtain an exact solution in 2D spherical coordinates for the velocity field after the shocked layer:

$$v_\phi(r_s) = \frac{4v_{z|u}}{(\gamma+1)} \frac{(M_n^2 - 1) |\cos \phi|}{M_n^2 [2 + (\gamma - 1) M_n^2]} \quad (3)$$

where ϕ is a polar angle and. We see that the azimuthal component of velocity after the shock becomes negative, and the polar component in the downstream region acquires a positive value: thus, a *backflow* develops.

2.3. The flow along the bow shock

After the HS, the backflow enters into the inner part of the bow shock (Figure 1), and the magnitude of the rotation is determined by the conservation law for vorticity in 2D:

$$\frac{|\omega|}{\rho} = \text{const} \quad (4)$$

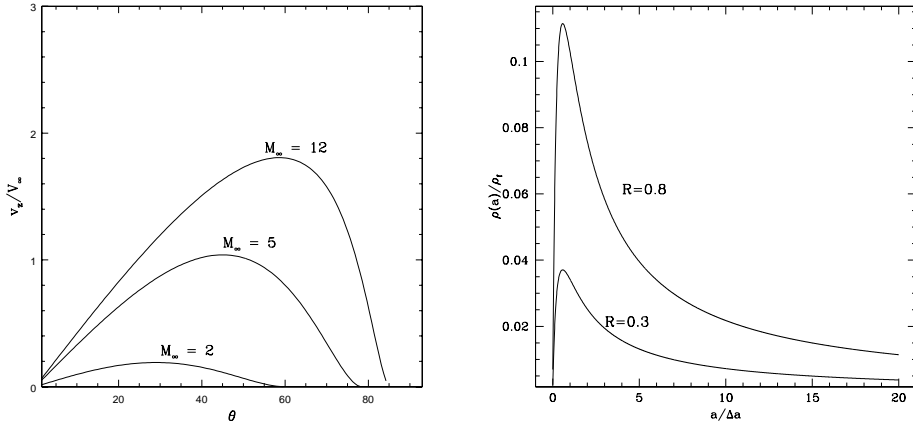


Figure 2. *Left:* The excursion of $|v_d|_z/v_{u|z}|$, as measured in eq. 3, for different values of the upstream Mach number. The flows within the cocoon usually are transonic, with $M_\infty \simeq 1 - 2$. *Right:* The scaled density within the bow shock as a function of $a/\Delta a$, the semi-major axis measured in units of the width of the spheroidal shell containing the shock. We plot the ratio $\rho/(3\rho_0 a_0^2/(\Delta a)^2)$, for two different values of the aspect ratio R .

Thus, in order to determine $|\omega|$, we have to determine the density inside the bow shock. Assuming that all the matter which was inside the cocoon is compressed within the bow shock, the final result reads:

$$\rho_{bs} = 3\rho_0 \left(\frac{a_0}{\Delta a} \right)^2 g(R) \frac{\lambda}{3\lambda^2 + 3\lambda + 1} \quad (5)$$

where ρ_0 is the central density of the galaxy halo, and we have defined: $\lambda = a_i/\Delta a$, where $a_i, \Delta a$ are the semimajor axis and the width of the bow shock, respectively. Note that the time-dependance of the density enters through the semi-major axis ($a \equiv a(t)$). Integrating eq. 5 we obtain the velocity along the bow shock, v_ϕ : the result is shown in Fig. 3 (*left*). We again notice that the maximum variations are always around unity, along the streamlines, and the velocity tends to decrease or to stay almost constant, as we approach the polar regions.

In summary, our model makes a few predictions. First, at least during the initial phases of the expansion, a circulation arises inside the cocoon, induced by the presence of a high density and entropy region (the Hot Spot). The backflow which develops tends to follow the bow shock, and then bends back near the meridional axis, perpendicular to the jet. For symmetry reasons, this flow will converge back towards the jet.

2.4. Numerical simulations

The numerical simulations confirm the numerical model sketched (Fig. 3, *right*). It is interesting to observe that the agreement with the model predictions is quite satisfactory, for a wide range of central densities and jet's injection powers. Note that in these simulations the main parameters like central halo mass,

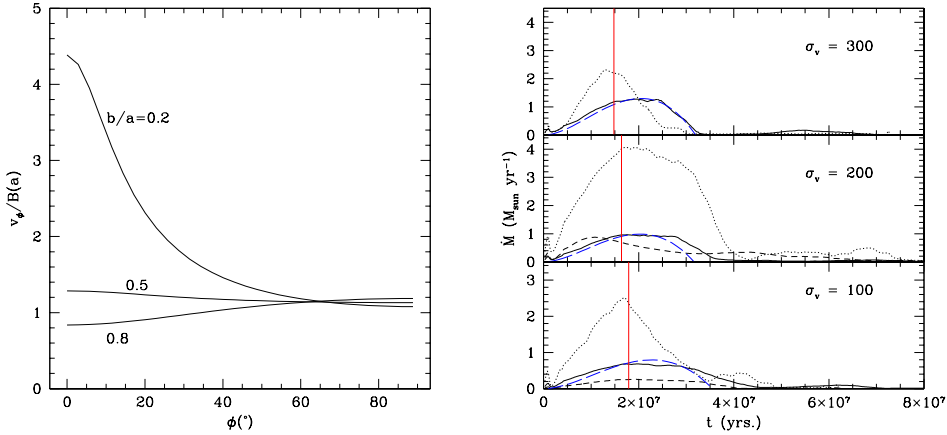


Figure 3. (Left): Velocity along the bow shock, for different aspect ratios. (Right): Mass inflow rates around a central disk region. The continuous lines are for simulations $s(100,200,300)av$, dotted lines for $s(100,200,300)p1$, dashed lines for $s(100,200,300)m1$. The dashed lines are the fits from the model given in the text. The red vertical lines mark the epoch when the reconfinement shock is destroyed and the jet starts to propagate freely, being only confined by the cocoon's ram pressure.

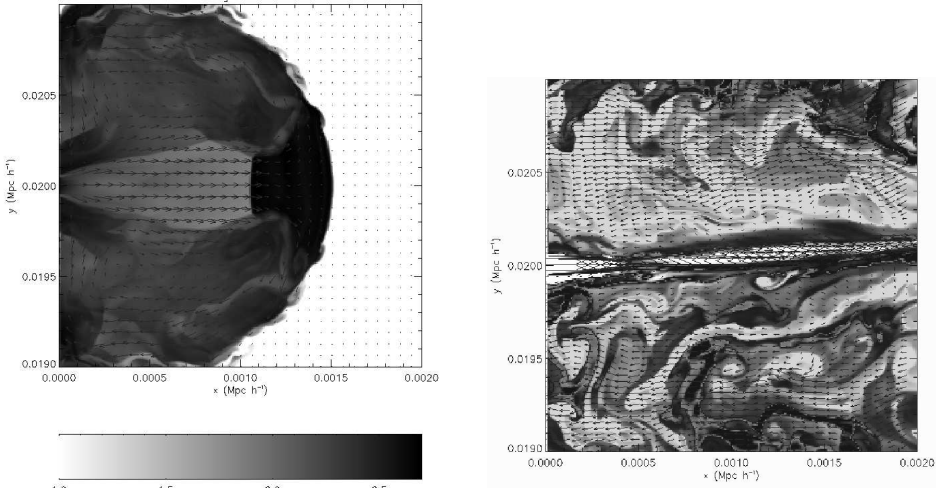


Figure 4. (Left): Velocity field before the destruction of the jet's shock by KH instabilities. The general pattern is well described by the model sketched in this paper. (Right): pattern of the flow after the disappearance of the shock along the jet. Note that the colour scale (not shown) is much smaller than in the figure on the right, thus density differences are in reality very small.

BH mass, jet's injection power, are chosen according to scaling relations (see Antonuccio-Delogu and Silk, 2008, for details).

The simulations also show that two different circulation regimes describe the flow within the cocoon (see Fig. 4). The presence of the shock before the HS

determines a flow similar to that described in our model. However, after a while this shock is destroyed by Kelvin-Helmholtz instabilities, and the hotspot propagates freely (Fig. 4, *right*). The gas near the jet is now reflected by the HS, and determines a counterstreaming flow which propagates back towards the central disc. The net mass inflow rate is however much less.

3. Conclusion

Realistic simulations of the flow pattern within an expanding cocoon show that a *backflow* develops soon after the cocoon forms. This determines a coherent flow towards the central parts of the AGN, whose magnitude is of the order of few $M_{\odot} \text{ yr}^{-1}$, i.e. the right order to feed the AGN and sustain its activity. A more detailed investigation of the consequences of this backflow is presented elsewhere (Antonuccio-Delogu and Silk, 2009, submitted).

Acknowledgments. The work of V.A.-D. has been supported by the European Commission, under the VI Framework Program for Research & Development, Action “*Transfer of Knowledge*” contract MTKD-CT-002995 (“*Cosmology and Computational Astrophysics at Catania Astrophysical Observatory*”). V.A.-D. would also express his gratitude to the staff of the subdepartment of Astrophysics, Department of Physics, University of Oxford, for the kind hospitality during the completion of this work.

References

Alexander P., 2006, MNRAS, 368, 1404
 Antonuccio-Delogu V., Silk J., 2008, MNRAS, 389, 1750
 Cap F., 2001, Sitzungsber. Abt. II, Österr. Akad. Wiss., Math.-Naturwiss. Kl., 210, 25
 Davies R. I., Mueller Sánchez F., Genzel R., Tacconi L. J., Hicks E. K. S., Friedrich S., Sternberg A., 2007, ApJ, 671, 1388
 Falle S. A. E. G., 1991, MNRAS, 250, 581
 González Delgado R. M., Cid Fernandes R., 2005, in de Grijs R., González Delgado R. M., eds, Starbursts: From 30 Doradus to Lyman Break Galaxies Vol. 329 of Astrophysics and Space Science Library, Starbursts in Low Luminosity Active Galactic Nuclei, pp 263–+
 Kaiser C. R., Alexander P., 1997, MNRAS, 286, 215
 Kaviraj S., Khochfar S., Schawinski K., Yi S. K., Gawiser E., Silk J., Virani S. N., Cardamone C. N., van Dokkum P. G., Urry C. M., 2008, MNRAS, 388, 67
 Kaviraj S., Kirkby L. A., Silk J., Sarzi M., 2007, MNRAS, 382, 960
 Sarzi M., Allard E. L., Knapen J. H., Mazzuca L. M., 2007, MNRAS, 380, 949
 Schawinski K., Khochfar S., Kaviraj S., Yi S. K., Boselli A. e. a., 2006, Nat, 442, 888
 Shapiro A., 1958, Z. Ang. Mathematik und Physik, 9, 637
 Silk J., Rees M. J., 1998, A&A, 331, L1
 Storchi-Bergmann T., González Delgado R. M., Schmitt H. R., Cid Fernandes R., Heckman T., 2001, ApJ, 559, 147
 Sutherland R. S., Bicknell G. V., 2007, ApJS, 173, 37
 Tortora C., Antonuccio-Delogu V., Kaviraj S., Silk J., Romeo A. D., Becciani U., 2009, MNRAS, 396, 61
 Yi S. K., Kaviraj S., Schawinski K., 2007, in Revista Mexicana de Astronomia y Astrofisica Conference Series Vol. 28 of Revista Mexicana de Astronomia y Astrofisica Conference Series, The Star Formation History of Early-type Galaxies. pp 109–112